Molecular Therapy
Methods & Clinical Development
Original Article

Development of capsid- and genome-modified optimized AAVrh74 vectors for muscle gene therapy

Jakob Shoti,[1] Keyun Qing,[1] Geoffrey D. Keeler,[1] Dongsheng Duan,[2] Barry J. Byrne,[3,4,5] and Arun Srivastava[1,4,5]

[1]Division of Cellular and Molecular Therapy, Department of Pediatrics, University of Florida College of Medicine, Gainesville, FL, USA; [2]Departments of Microbiology and Immunology, Neurology, Biomedical Sciences, and Chemical and Biomedical Engineering, University of Missouri, Columbia, MO, USA; [3]Child Health Research Institute, Department of Pediatrics, University of Florida College of Medicine, Gainesville, FL, USA; [4]Department of Molecular Genetics and Microbiology, University of Florida College of Medicine, Gainesville, FL, USA; [5]Powell Gene Therapy Center, University of Florida College of Medicine, Gainesville, FL, USA

The first generation of adeno-associated virus (AAV) vectors composed of the naturally occurring capsids and genomes, although effective in some instances, are unlikely to be optimal for gene therapy in humans. The use of the first generation of two different AAV serotype vectors (AAV9 and AAVrh74) in four separate clinical trials failed to be effective in patients with Duchenne muscular dystrophy, although some efficacy was observed in a subset of patients with AAVrh74 vectors leading to US Food and Drug Administration approval (Elevidys). In two trials with the first generation of AAV9 vectors, several serious adverse events were observed, including the death of a patient in one trial, and more recently, in the death of a second patient in an N-of-1 clinical trial. In a fourth trial with the first generation of AAVrh74 vectors, myositis and myocarditis were also observed. Here, we report that capsid- and genome-modified optimized AAVrh74 vectors are significantly more efficient in transducing primary human skeletal muscle cells *in vitro* and in all major muscle tissues *in vivo* following systemic administration in a murine model. The availability of optimized AAVrh74 vectors promises to be safe and effective in the potential gene therapy of muscle diseases in humans.

INTRODUCTION

Recombinant adeno-associated virus (AAV) vectors have been and are currently being used as a gene-delivery vehicle for gene therapy of a wide variety of monogenetic human diseases.[1–3] With 309 Phase I/II/III clinical trials to date, and 5 US Food and Drug Administration (FDA)–approved AAV-based therapies (Luxturna, Zolgensma, Hemgenix, Elevidys, and Roctavian), this technology is at the forefront of the gene therapy landscape.[4,5] However, it has become increasingly clear that there are two major limitations of the first generation of AAV vectors: (1) the naturally occurring capsids trigger an immune response, especially at high doses, and (2) the single-stranded genome that is currently used in most of the AAV vectors is transcriptionally less efficient.[6] More specifically, in a number of clinical trials, it has been documented that the administration of high vector doses induces a host cytotoxic T lymphocyte immune response to capsid proteins.[7,8] At the clinical level, this immune response results in the clearance of target cells expressing the therapeutic gene, as well as serious adverse events (SAEs) in patients. Recently, the use of the first generation of AAV8 vectors in a Phase I/II trial for X-linked myotubular myopathy (XLMTM) resulted in 3 deaths at a high dose of 3×10^{14} vg/kg, and an additional death even at a lower dose of 1.3×10^{14} vg/kg.[9] These findings underscore the need for the development of more efficient AAV vectors that could be administered to patients at lower doses without compromising clinical efficacy. In addition, the use of single-stranded AAV (ssAAV) vectors, which are transcriptionally less efficient, is necessary for the gene therapy of Duchenne muscular dystrophy (DMD), given the large size of the dystrophin gene.

Several gene therapy trials for DMD have been or are currently being performed using various AAV serotype vectors.[3,10] A chimeric AAV capsid variant, AAV2.5, composed of the AAV2 capsid with 5 mutations from the AAV1 capsid, was first used in a Phase I clinical trial for DMD and was found to be safe and well tolerated, but no clinical efficacy was achieved.[11] In a Phase I/II clinical trial sponsored by Solid Biosciences using AAV9 vectors, adverse events such as complement activation and thrombocytopenia causing kidney injury and cardiopulmonary insufficiency were reported, although more recent data showed clinical improvements.[12] In a trial sponsored by Pfizer, also using AAV9 vectors, several SAEs occurred such as acute kidney injury involving atypical hemolytic uremic syndrome and thrombocytopenia and the death of a patient at a high dose of 2×10^{14} vg/kg.[13] More recently, the death of a patient was reported in an N-of-1 clinical trial sponsored by Cure Rare Disease using AAV9-CRISPR.[14] Sarepta Therapeutics reported the results of its Phase I/II trial using AAVrh74 vectors. Manageable adverse events (e.g., nausea, vomiting) were observed in all of the participants in the active cohort, yet the study failed to meet its primary functional endpoint.[15] However, in a post

Received 4 March 2023; accepted 31 October 2023;
https://doi.org/10.1016/j.omtm.2023.101147.

Correspondence: Arun Srivastava, Division of Cellular and Molecular Therapy, Department of Pediatrics, University of Florida College of Medicine, Gainesville, FL, USA.
E-mail: aruns@peds.ufl.edu

hoc analysis, patients at 4 to 5 years of age showed statistically significant clinical improvement, leading to the FDA approval of SRP-9001 (Elevidys) for this age group of patients.[16] However, Elevidys failed to meet primary end point in a recent Phase III trial. Based on the initial findings of improvement in timed function tests, there is an ongoing interest in achieving greater efficacy with next-generation AAV capsid derivatives and new vector genome designs. The goal of these refinements is to achieve therapeutic levels of the dystrophin protein at a significantly lower dose of AAVrh74 vectors.

In our previously published studies with AAV2 serotype vectors in which we performed site-directed mutagenesis of specific surface-exposed amino acid residues, the resulting next generation (NextGen) of vectors were observed to be up to 10-fold more efficient in the mouse liver at a 1-log lower dose,[17,18] and less immunogenic[19] than their wild-type (WT) counterpart. We have also reported that the extent of transgene expression from ssAAV vectors could be augmented up to ?8-fold by modifying the AAV genome to develop generation X (GenX) ssAAV vectors.[20] Furthermore, the combination of these strategies led to the development of optimized (Opt^X) AAV vectors, which were observed to be up to ?20- to 30-fold more efficacious in human cells *in vitro* and in mouse tissues *in vivo*.[21]

In the present study, we applied this two-pronged strategy to generate NextGen, GenX, and Opt^X AAVrh74 serotype vectors and evaluated their transduction efficiency in primary human skeletal muscle cells *in vitro* and in mouse muscle tissues *in vivo*. Further optimization of these vectors promises to lead to safer and more effective gene therapy of neuromuscular diseases in humans.

RESULTS

Development of capsid-modified NextGen AAVrh74 vectors

In our previously published studies, we identified several surface-exposed specific tyrosine (Y) and threonine (T) residues, the site-directed mutagenesis of which led to a significant increase in the transduction efficiency of AAV2 serotype vectors.[17,18,22] When two Y residues (Y444F, Y730F) were combined with a T residue (T492) to generate a triple-mutant (TM) AAV2 vector, its transduction efficiency was further increased significantly.[22] Interestingly, the sequence alignment of AAV2 and AAVrh74 capsids revealed that each of these corresponding amino acids was conserved (Figure S1A). In addition to generating the Y444F + Y733F + T494V TM-AAVrh74 vector, we also generated various single (Y447F; Y733F; N665R; T494V; K547R)-, triple (Y447F + 733F + N665R; Y447F + 733F + K547R)-, and pentuple (Y447F + 733F + N665R + T494V + K547R)-mutant AAVrh74 vectors (Figure S1B), and identified the Y447F + Y733F + T494V TM-mutant as the most efficient in transducing human HeLa cells *in vitro* (Figure S2). Consistent with our previously published studies with the TM-AAV2 vectors, the increased transduction efficiency of the TM-AAVrh74 vectors was also due to reduced ubiquitination and proteasome-mediated degradation, followed by improved intracellular trafficking and nuclear transport (Figure S3). The TM-mutant also showed the highest mean fluorescence intensity (Figure S2) and in murine hepatocytes even at 1- to 2-log lower doses (Figure S4), and it was used in all subsequent studies.

Development of genome-modified GenX AAVrh74 vectors

We have previously reported that encapsidation of the ssAAV genome in which one of the D-sequences in the inverted terminal repeats (ITRs) is replaced with a substitute (S)-sequence (shown schematically in Figure S5), into AAV2 capsids leads to vectors, called GenX, that mediate ?8-fold increased transgene expression compared with that from conventional ssAAV2 vectors.[21] In the present study, we generated GenX AAVrh74-cytomegalovirus (CMV)-humanized Renilla reniformis GFP (hrGFP) vectors and compared the extent of the transgene expression from these vectors, which was observed to be up to 5-fold higher than that from the WT-ssAAVrh74 vectors (Figure S6). Interestingly, the extent of the transgene expression from GenX AAVrh74 vectors was up to ~13-fold higher in primary human skeletal muscle cells (Figure S7).

Development of capsid+genome-modified Opt^X AAVrh74 vectors

As described previously with the AAV2 serotype,[22] Opt^X AAVrh74 vectors were generated by combining the NextGen capsid-modified (TM-AAVrh74) and GenX genome-modified GenX AAVrh74) into one vector. The transduction efficiency of the Opt^X AAVrh74 vectors was 4-fold higher than that of the WT AAVrh74 vectors in HeLa cells as determined by fluorescence microscopy (Figure S8) or flow cytometry (Figure S9).

Evaluation of the transduction efficiency of WT, TM, and Opt^X AAVrh74 vectors in primary human skeletal muscle cells *in vitro*

We next evaluated the transduction efficiency of WT, TM, and Opt^X AAVrh74-CMV-hrGFP vectors in primary human skeletal muscle cells. As can be seen in Figure 1A, Opt^X AAVrh74 vectors mediated higher levels of transgene expression at both 1,000 vg/cell and 3,000 vg/cell. Expression data were quantified using ImageJ analysis and represented as $pixels^2$ per visual field. Analyses revealed that Opt^X AAVrh74 vectors resulted in a ~5-fold higher expression level as compared with the WT AAVrh74 vectors (Figure 1B). The enhanced transduction efficiency of both TM and Opt^X vectors was not due to the increased entry of these vectors in primary human skeletal muscle cells because the total vector genome copy numbers per cell were not significantly different from those of the WT AAVrh74 vectors (Figure 1C).

Evaluation of the transduction efficiency of WT and Opt^X AAVrh74 vectors in mouse muscles *in vivo*

We first evaluated the efficacy of WT, TM, GenX, and Opt^X AAVrh74 vectors *in vivo* following direct intramuscular (i.m.) injections in the gastrocnemius (GA) muscle in C57BL/6 mice (N = 4 each). TM AAVrh74 vectors were ~10-fold more efficient (Figure S10), and GenX AAVrh74 vectors were ~8-fold more efficient (Figure S11) than their WT counterpart 2 weeks postinjections. Opt^X AAVrh74 vectors were ~2-fold more efficient than TM AAVrh74 vectors (Figure S12). In the next set of experiments, to more closely mimic the

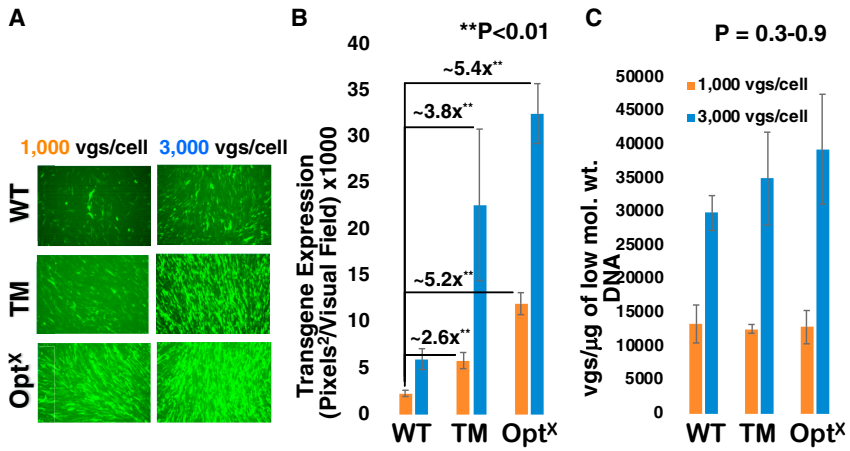

Figure 1. Transduction efficiency of WT, TM, and Opt^X AAVrh74 vectors in primary human skeletal muscle cells *in vitro*

(A) Primary human skeletal muscles were transduced in triplicate at 1,000 and 3,000 vg/cell, and transgene expression was visualized under a fluorescence microscope 72 h post-transduction. (B) Data were quantitated using the NIH ImageJ software. (C) Total vector genome copy numbers were quantitated by qPCR assays using hrGFP primers and reported as vector genomes per microgram of extrachromosomal DNA. Statistical significance was determined between WT and TM, WT and Opt^X vectors using the Student's t test. Error bars and p values are indicated. mol. wt., molecular weight.

clinical scenario, 1×10^{12} vg each of WT and Opt^X AAVrh74 vectors were delivered systemically in C57BL/6 mice (N = 6 each) by tail vein injections. Eight weeks postinjections, tibialis anterior (TA) and GA muscles were harvested, sectioned, and evaluated for transgene expression using fluorescence microscopy. These results are shown in Figure 2A. As can be seen, the transduction efficiency of Opt^X AAVrh74 was ~4- and ~6-fold higher than the WT AAVrh74 vectors in TA and GA muscles, respectively (Figure 2B). Total vector genome copy numbers were also determined in TA and GA muscles, in addition to those in liver, diaphragm, and heart tissues from each mouse. These results, shown in Figure 2C, indicate that whereas a substantial fraction of both vectors was sequestered in the liver, an observation previously reported by others,[23] the vector genome copy numbers of both WT and Opt^X AAVrh74 were not significantly different in any of the tissues analyzed. These data are consistent with our previously published studies that the increased transduction efficiency of Opt^X AAVrh74 vectors is due to improved intracellular trafficking and nuclear transport.[17,24]

We evaluated the extent of the hrGFP expression in liver, diaphragm, and heart tissues at the RNA level using qRT-PCR assays. These results are shown in Figure 3. As can be seen, the delta-delta analyses, relative to the WT AAVrh74 vector control, revealed that the extent of the transgene expression from the Opt^X AAVrh74 vectors was significantly higher in the liver and diaphragm, but not in the heart. The delta-delta analyses, relative to the PBS control, also revealed that the extent of the transgene expression from the Opt^X AAVrh74 vectors was significantly higher in the liver and diaphragm, but not in the heart (Figure S13).

Development of, and transgene expression from, GenY AAVrh74 vectors

To further augment the extent of transgene expression from an ssAAV genome, we replaced the distal 10 nt in the D-sequence in the left ITR with a consensus full-length glucocorticoid receptor-binding element (GRE) to create a generation Y (GenY) ssAAV vector, shown schematically in Figure S14. This was based on our previous observation that the distal 10 nt in the D-sequence share partial homology to the GRE $^1/_2$ site, and that replacement of the distal 10 nt in the D-sequence with a consensus full-length GRE in an self-complementary AAV2 (scAAV2) vector genome significantly increases the transgene expression.[25]

The extent of the transgene expression from WT and GenY AAVrh74 vectors was evaluated in HeLa cells (Figure S15). A modest ~2-fold increase was observed. We also evaluated the extent of the transgene expression from WT and GenY AAVrh74 vectors in the mouse muscle cell line C2C12 (Figure S16) in the absence and presence of tyrphostin, known to promote AAV second-strand DNA synthesis.[26] As can be seen in Figure S16, the extent of transgene expression from GenY AAVrh74 vectors was up to ~5-fold higher in C2C12 cells pretreated with tyrphostin.

We also evaluated the transduction efficiency of WT, GenX, and GenY AAVrh74 vectors in primary human skeletal muscle cells. As shown in Figures 4A and 4B, at 3,000 vg/cell, transgene expression from GenY AAVrh74 vectors was ~6-fold higher than that from the WT AAVrh74 vectors. Again, the increased transgene expression from both GenX and GenY AAVrh74 vectors was not due to the increased entry of these vectors because the total vector genome copy numbers per cell were not significantly different from those of the WT AAVrh74 vectors (Figure 4C).

Evaluation of the transduction efficiency of TM and Opt^Y AAVrh74 vectors in mouse muscles *in vivo*

GenY genomes were packaged into TM capsids to generate Opt^Y AAVrh74 vectors, and the transduction efficiency of these vectors was evaluated in mouse TA and GA muscles following systemic delivery in C57BL/6 mice (N = 6 each). Transgene expression was evaluated 8 weeks postinjections. These results, shown in Figure 5, indicated that compared with the TM vectors, transgene expression from the Opt^Y vectors in both TA and GA muscles was higher, albeit not statistically significant (Figure 5B).

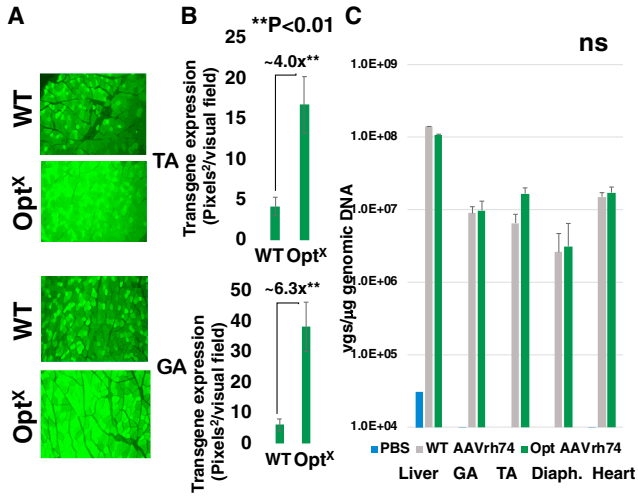

Figure 2. Transduction efficiency and biodistribution of WT, TM, and Opt^X AAVrh74 vectors in primary murine muscles *in vivo*

(A) Each vector was injected intravenously at 1×10^{12} vg/mouse, and transgene expression in TA and GA skeletal muscle sections was visualized under a fluorescence microscope 8 weeks postinjection. (B) Data were quantitated using the ImageJ software. (C) Total vector genome copy numbers were analyzed in various tissues by qPCR assays using hrGFP primers and reported as vector genomes per microgram of genomic DNA on a logarithmic scale. Statistical significance was determined between WT and OptX using Student's t test. Error bars and p values are indicated. Diaph., diaphragm; ns, not significant.

We also evaluated the extent of the transgene expression in mouse liver, heart, diaphragm, and skeletal muscles (GA and TA) at the RNA level. The delta-delta analysis, relative to the TM AAVrh74 vector control, indicated that the extent of the transgene expression from the Opt^Y AAVrh74 vectors was significantly higher in each of the muscle tissues, but not in the liver (Figure 6). Similarly, the delta-delta analysis, relative to the PBS control, indicated that the extent of the transgene expression from the Opt^Y AAVrh74 vectors was significantly higher in each of the muscle tissues, but not in the liver (Figure S17).

DISCUSSION

Because AAV evolved as a virus and not as a vector for the purposes of delivery of therapeutic genes, it has become increasingly clear that the first generation of AAV vectors, although efficacious in certain immune-privileged organs such as eye (Luxturna) and brain (Zolgensma), can be further optimized by the approach demonstrated here.[6,27] It is also becoming clear that the host immune response to the first generation of AAV vectors correlates directly with the vector dose. Cogent examples of this include the reported deaths of 3 patients in a gene therapy trial of XLMTM at a high dose of 3×10^{14} vg/kg and the death of a patient at a lower dose of 1.3×10^{14} vg/kg using the first generation of AAV8 vectors.[9] Similarly, the death of a patient was recently reported in a gene therapy trial of DMD at a high dose of 1×10^{14} vg/kg of the first generation of AAV9 vectors.[14] Because the estimated total number of cells in a "reference human" of 70 kg has been reported to be ~30 trillion,[28] a vector dose of 3×10^{14} vg/kg (21 quadrillion) would be ~700 times the total number of cells in the body in the XLMTM trial. Even with a lower dose of 1×10^{14} vg/kg (7 quadrillion), the vector dose would still be ~234 times the total number of cells in the body in the DMD trial, remarkably high numbers indeed. However, this theoretical dose comparison is much more complicated than *in vivo* biodistribution, but following systemic delivery of any AAV vector given in excess of 1×10^{14} vg/kg leads to viremia at a level never reached by a natural infection. The innate and adaptive response to such a DNA and protein load has reached the maximum tolerated dose.

For nearly 2 decades, we have expended significant effort to focus on the limitations of the first generation of recombinant AAV vectors and the circumvention of these limitations to develop novel AAV vectors that are capable of (1) high-efficiency transduction, (2) efficient transgene expression, and (3) less immunogenicity. We have approached this issue from multiple angles. First, by modifying the AAV capsid protein, we developed the NextGen of AAV vectors, which are up to 10-fold more efficacious at reduced doses.[17,18] These capsid modifications do not affect tissue tropism or receptor/co-receptor binding, but rather improve intracellular trafficking and nuclear transport by significantly reducing the ubiquitination and proteasome-mediated degradation of the vector.[17,24] These vectors are also less immunogenic.[19] Second, we modified the AAV vector genome to develop the GenX AAV vectors that mediate up to an 8-fold enhanced transgene expression.[20] Third, we combined both strategies to generate the optimized Opt^X AAV serotype vectors that are ~20- to 30-fold more efficient at further reduced doses.[21] In the present study, we extended these approaches to include the development of GenY and Opt^Y AAV vectors and applied these strategies to the AAVrh74 serotype, which is known to have efficient tropism for human skeletal and cardiac muscle tissues and has been shown to possess an excellent safety profile in the gene therapy of DMD.[29]

Studies have shown that ~90% of DMD patients will succumb to respiratory failure and/or cardiomyopathy.[30,31] An ideal AAV vector for DMD gene therapy must be competent at transducing a patient's entire skeletal muscle system as well as the diaphragm and the heart. The systemic administration of Opt^X and Opt^Y AAVrh74 vectors in C57BL/6 mice led to a significant increase in the transduction efficiency and transgene expression across all of the muscle tissues evaluated. Although protein-level data were not obtained from the heart and the diaphragm, the high levels of vector genomes and mRNAs were detectable in these tissues.

Thus, the clinical significance of this study is directly related to the potential gene therapy of DMD. In the present study, we developed optimized AAV vectors based on the AAVrh74 serotype to provide an improved iteration that is capable of disease remediation with reduced doses as compared to high vector doses currently being administered in DMD clinical trials. Our capsid and genome modifications (summarized in Table S1) significantly increased the transduction profile of AAVrh74 across various organs following systemic

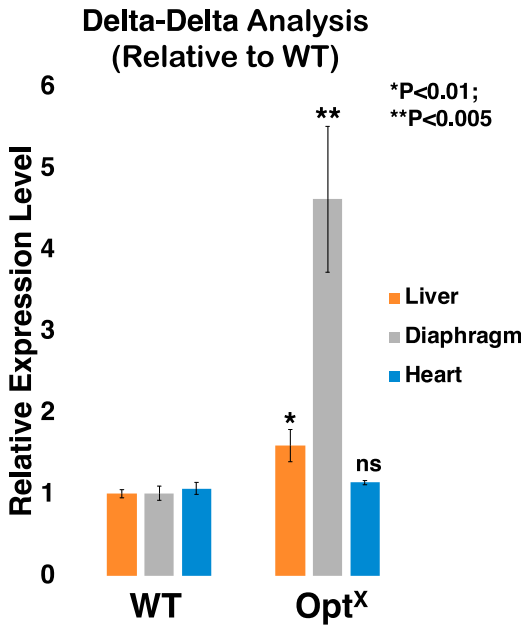

Figure 3. Transgene expression from WT and Opt^X AAVrh74 vectors in primary murine muscles *in vivo*

Total RNA samples isolated from liver, diaphragm, and heart at 8 weeks post-injection were subjected to RT-PCR-qPCR and analyzed by ΔCt = (hrGFP Ct – β-actin Ct). Results are reported as relative expression level or $2^{-\Delta\Delta CT}$ relative to WT-AAVrh74 vectors, as described in materials and methods. Bar graph represents the respective average of WT- and Opt^X-AAVrh74 ΔCt across organs. Statistical significance was determined between WT and OptX, respective of organ, using the Student's t test. Error bars and p values are indicated.

administration in murine models. Interestingly, none of the modifications made redirected the AAVrh74 vectors away from targeted tissues. However, following systemic administration, a large fraction of the vectors was sequestered in the liver, effectively reducing the bioavailability for muscle transduction. This warrants the development of liver detargeted Opt^X and Opt^Y AAVrh74 vectors. Future studies will explore further refinement of these vectors to detarget from the liver to reduce liver sequestration and increase muscle tissue transduction.

Although our present study was underway, two independent groups reported the development of novel myotropic AAV vectors—AAVMYO[32,33] and MyoAAV.[34] These vectors were derived from shuffled AAV library and directed evolution. Although a significant step forward, both vectors are based on AAV9 and they also contain an arginine-glycine-aspartic acid motif, a specific ligand for integrins. The efficacy AAVMYO has been documented in normal mice and mdx mice and that of MyoAAV in both normal and mouse models of DMD and XLMTM, as well as in nonhuman primates (NHPs). However, it still remains to be seen whether these vectors will prove to be safe in clinical trials, given the potential for the creation of hitherto unknown T and B cell antigenic epitopes, which may be tolerated in animal models, but not in humans. In this context, it is noteworthy that in gene therapy trials with the first generation of AAV serotype vectors, none of the immune responses was observed in murine, canine, or NHP models, as was observed in patients with hemophilia.[35–38] Furthermore, given the SAEs observed in 4 different clinical trials with AAV vectors derived from directed evolution,[39–42] it remains to be seen whether AAVMYO or MyoAAV vectors would prove to be safe in the gene therapy of DMD in humans.[43]

There are 2 limitations in our present study. First, all of the data generated are from AAVrh74 vectors expressing a reporter gene rather than a therapeutic gene, which will be pursued in our future studies. Second, although the efficacy of both Opt^X and Opt^Y AAVrh74 vectors was documented in primary human skeletal muscle cells *in vitro*, the efficacy of these vectors was limited to murine muscles *in vivo*. Our current plans include additional studies in a mouse model of DMD, and in future studies, in a canine model of DMD, followed by safety studies in NHPs.

MATERIALS AND METHODS

Cell lines, primary human cells, cell cultures, and reagents

HEK293, HeLa, and C2C12 were purchased from American Type Culture Collection (ATCC, Manassas, VA) and maintained at 37°C in 5% CO_2 in DMEM (Lonza, Walkersville, MD) supplemented with 10% fetal bovine serum (FBS; Sigma, St. Louis, MO) and 1% penicillin-streptomycin (Invitrogen, Grand Island, NY). Primary human skeletal muscle cells (spindle shaped, elongated, nondifferentiated), isolated from normal human skeletal muscle, were also purchased from ATCC (catalog no. PCS-950-010), and maintained at 37°C in 5% CO_2 in mesenchymal stem cell basal medium supplemented with 10% FBS and 1% penicillin-streptomycin.

Site-directed mutagenesis of surface-exposed amino acid residues in AAVrh74 capsids

A 2-stage procedure, based on QuikChange II site-directed mutagenesis (Agilent Technologies) was performed by using plasmid pACG-Crh74.[44] Briefly, in stage 1, 2 PCR extension reactions were performed in separate tubes for each mutant. One tube contained the forward PCR primer and the other contained the reverse primer. In stage 2, the 2 reactions were mixed, and a standard PCR mutagenesis assay was carried out per the manufacturer's instructions. PCR primers were designed to introduce changes from tyrosine to phenylalanine, asparagine to arginine, threonine to valine, and lysine to asparagine residues and a silent change to create a new restriction endonuclease site for screening purposes. All of the mutants were screened with the appropriate restriction enzyme and were sequenced before use.

Viral vector production

Vectors were either packaged in-house or by PackGene (Worcester, MA). Briefly, WT ssCMVp-hrGFP, or GenX ssCMVp-hrGFP genomes were packaged into WT or mutated-AAVrh74 capsids using the triple-plasmid transfection method, mediated by polyethyleneimine 50 (PEI; linear, molecular weight 25,000; Polysciences, Warrington, PA). Briefly, HEK293 cells were cotransfected with three plasmids using PEI, and medium was replaced at 6 h posttransfection. Cells were

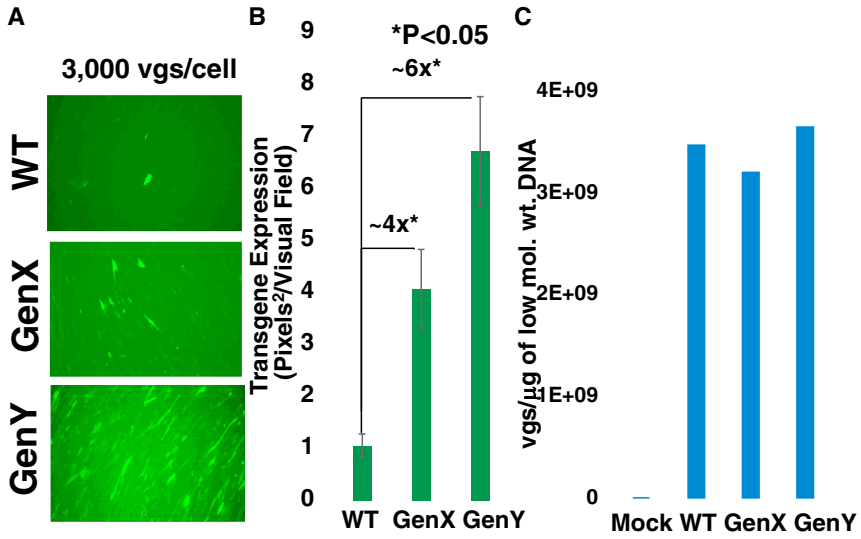

Figure 4. Transduction efficiency of WT, GenX, and GenY AAVrh74 vectors in primary human skeletal muscles cells *in vitro*

(A) Primary human skeletal muscle cells were transduced with 3,000 vg/cell of each vector, and transgene expression was visualized 72 h posttransduction. (B) Quantification of fluorescence intensity using the ImageJ software. (C) Total vector genome copy numbers were quantitated by qPCR assays. Statistical significance was determined between WT and GenX, and WT and GenY vectors using the Student's t test. Error bars and p values are indicated.

harvested at 72 h posttransfection, subjected to 3 rounds of freeze-thawing, and then were digested with 100 U/mL Benzonase (EMD Millipore, Darmstadt, Germany) at 37°C for 1 h. Viral vectors were purified by iodixanol (Sigma) gradient ultracentrifugation followed by ion-exchange chromatography using HiTrap Q HP (GE Healthcare, Piscataway, NJ), washed with PBS, and concentrated by centrifugation using centrifugal spin concentrators with a 150,000-molecular-weight cutoff. Viral vectors were resuspended in 500 µL PBS. Titers were determined by qRT-PCR assays, as previously described.[45,46]

AAV transduction assays *in vitro*

Approximately 1×10^5 HeLa and C2C12 cells or 5×10^5 primary human skeletal muscle cells were plated in triplicate in 12-well plates and incubated at 37°C for 24 h. Cells were washed once with PBS and then transduced at 37°C for 2 h with recombinant WT AAVrh74 or mutant AAVrh74 vectors as described previously.[47,48] Cells were incubated in complete DMEM containing 10% FBS and 1% antibiotics/antimycotic for 72 h. Transgene expression was evaluated as follows.

Fluorescence microscopy

Transduction efficiency was measured by hrGFP fluorescence imaging using a Leica DM IRB/E fluorescence microscope (Leica Microsystems Wetzlar GmbH, Wetzlar, Germany). For *in vitro* samples, complete media was removed and replenished with PBS, followed by image acquisition with 3–5 images per well of mock-infected and vector-infected cells at 100× magnification. For *in vivo* tissue slide imaging, light and dark visual fields were acquired to ensure ? 100% cell coverage for proper comparison assessment with 5–6 dark visual field images per slide at 100× magnification. All of the images were analyzed quantitatively by ImageJ analysis software (NIH, Bethesda, MD). Transgene expression was assessed as the total area of green fluorescence (pixel^2) per visual field, and bar graphs were generated representing the mean ± SEM.

Flow cytometric analysis

Transduced cells were washed 1× with PBS, trypsinized, and resuspended using complete media at 72 h postinfection. Suspended cells were then pelleted by centrifuge at 5,000 rpm for 5 min. Cell pellets were washed with PBS 1× and then resuspended in 500 µL of ice-cold PBS and placed on ice. Cells were analyzed using the flow cytometer Accuri C6 (BD Biosciences, Franklin Lakes, NJ) for 100,000 events and followed by processing with the software package FCS Express 6 Flow.

Isolation of low-molecular-weight DNA

Nuclear DNA fractions from HeLa, C2C12, and human primary cells were isolated using Hirt's solution (10 mM Tris, pH 7.9, 10 mM EDTA, 0.6% SDS). Briefly, transduced and mock-transduced cells were washed with ice-cold PBS followed by incubation with 1 vol of Hirt's solution. Cells were then scraped from the plate and decanted into tubes. Roughly 0.2 vol of 5 M NaCl was added to each tube to precipitate genomic DNA and placed at 4°C overnight. The following day, cell debris was pelleted by centrifuge at 13,000 rpm for ?1 h at 4°C. The supernatant (600 µL) was decanted into a new tube and phenol-chloroform extracted and ethanol precipitated as described previously.[8]

qPCR assay

Extrachromosomal DNA, cDNA samples, and standards were serial diluted and subjected to qPCR using PowerUp Sybr Green 2× Mix (Thermo Fisher Scientific, Waltham, MA), qPCR primers (EuroFins, Luxembourg, Luxembourg), and C1000 CFX96 Real-Time System (Bio-Rad, Hercules, CA). Standards were linearized plasmids for the respective gene cassette of known masses as determined by NanoDrop Lite (Thermo-Fisher Scientific). Quantitation analysis was conducted using Microsoft Excel to generate standard curves and determine gene copy numbers. For delta-delta relative mRNA expression analysis, cDNA samples were subjected to qPCR with hrGFP reporter gene (forward: 5′-gtggtgtacatgaacgacgg-3′; reverse: 5′-cctggagaagacctacgtgg-3′), and housekeeping (β-actin) gene (forward: 5′-acacccgccaccagttc-3′; reverse: 5′-tacagcccggggag-cat-3′, individually, and subsequent Cts were then used for data analysis.

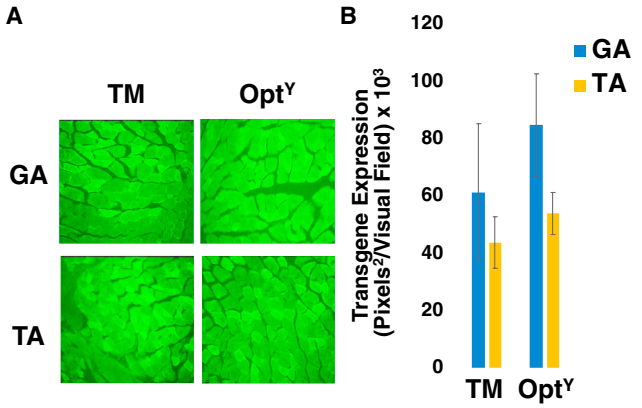

Figure 5. Transduction efficiency of TM and Opt^{Y} AAVrh74 vectors in primary murine muscles *in vivo*

(A) Each vector was injected intravenously at 1 × 10^{12} vg/mouse, and transgene expression in TA and GA skeletal muscle sections was visualized under a fluorescence microscope 8 weeks postinjection. (B) Data were quantitated using ImageJ software. Error bars are indicated.

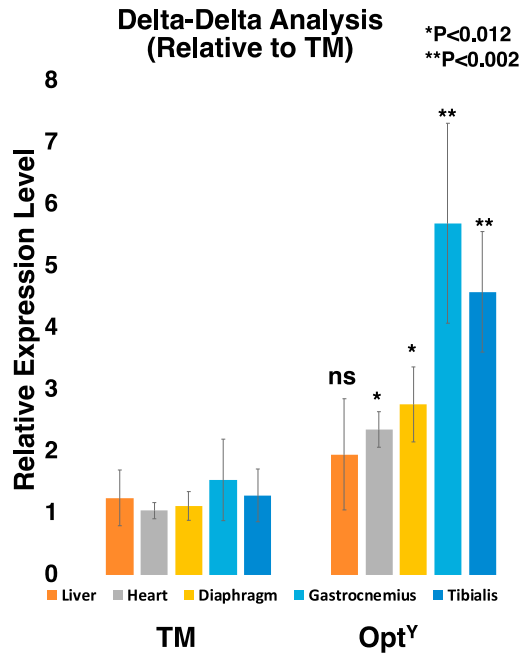

Figure 6. Transgene expression from TM and Opt^{Y} AAVrh74 vectors in primary murine muscles *in vivo*

Total RNA samples isolated from various organs were subjected to RT-PCR-qPCR and analyzed by ΔCt = (hrGFP Ct – β-actin Ct) respective average of Opt^{Y}-AAVrh74 ΔCt and reported as relative expression level or $2^{-\Delta\Delta CT}$ relative to TM-AAVrh74 vectors, as described in materials and methods. Statistical significance was determined between TM and Opt^{Y} AAV vectors using the Student's t test. Error bars and p values are indicated.

Preparation of whole-cell lysates (WCLs) and coimmunoprecipitations

WCLs were prepared as described previously,[24,49] with the following modifications. Briefly, 2 × 10^{6} HeLa cells were either mock-treated or treated with 4 μM MG132 for 2 h and then were infected with TM AAVrh74 vectors at 1 × 10^{4} vg/cell for 2 h at 37°C. For immunoprecipitations, at 4 h postinfection, cells were treated with 0.25% trypsin and washed extensively with PBS to remove any unabsorbed virus particles. Then, they were resuspended in 1 mL hypotonic buffer (20 mM HEPES, pH 7.5, 5 mM KCl, 0.5 mM $MgCl_2$) containing 1 mM DTT, 10 mM NaF, 2 mM Na_3VO_4, 0.5 mM PMSF, 10 μg/mL aprotinin, and 10 μg/mL leupeptin. WCLs were prepared by homogenization in a tight-fitting Duval tissue grinder until ?95% cell lysis was achieved as monitored by trypan blue dye exclusion assay. WCLs were cleared of nonspecific binding by incubation with 0.25 mg of normal mouse immunoglobulin G (IgG) together with 20 μL of protein G plus agarose beads for 60 min at 4°C in an orbital shaker. After preclearing, 2 μg of capsid antibody against intact AAV2 particles (A20) (mouse IgG3) was added and incubated at 4°C for 1 h, followed by precipitation with protein G agarose beads at 4°C overnight on shaker. Pellets were collected by centrifugation at 2,500 rpm for 5 min at 4°C and washed 4 times with PBS. After the final wash, supernatants were aspirated and discarded, and pellets were resuspended in equal volumes of 2× SDS sample buffer. Resuspended pellet solutions at 20 μL were used for western blotting with horseradish peroxidase (HRP)–conjugated anti-Ub antibody as described below. Western blotting was performed as described previously.[17,49,50] For immunoprecipitations, resuspended pellet solutions were boiled for 5 min and 20 μL of samples were used for SDS-PAGE. After blocking at 4°C overnight with 5% nonfat milk in 1× Tris-buffered saline, membranes were treated with monoclonal HRP-conjugated anti-Ub antibody (1:2,000 dilution). Immunoreactive bands were visualized using chemiluminescence substrate (SuperSignal West Pico Plus Chemiluminescent Substrate, Thermo-Fisher Scientific) and imaged with the Amersham Imager 680 (General Electric, Chicago, IL).

In vivo transduction analysis

Male C57BL/6 mice were purchased from The Jackson Laboratory (Bar Harbor, ME) and maintained in the University of Florida Animal Care Facility. All of the experimental protocols involving animals were approved by the Institutional Animal Care and Use Committee guidelines. For i.m. injections, 1 × 10^{9} vg (4 × 10^{10} vg/kg) of WT ssCMVp-hrGFP or GenX ssCMVp-hrGFP genomes packaged into WT or mutant AAVrh74 capsids were injected into the GA muscle in C57BL/6 mice (N = 4 per group). Two weeks postvector injections, mice were humanely euthanized and GA tissue was harvested, which was then cryosectioned and samples were placed on tissue slides. For tail vein injections, 1 × 10^{12} vg (4 × 10^{13} vg/kg) of WT, or Opt^{X} AAVrh74-CMVp-hrGFP vectors were injected into mice (N = 6 per group). At 8 weeks postinjection, mice were humanely euthanized and organs were harvested, which included the liver, heart, diaphragm, GA, and TA muscles. A portion of all of the organs were subjected to DNA and RNA isolation, whereas only the murine liver, GA, and TA were cryosectioned and placed on tissue slides. All of the slides were stored in −80°C until imaging, at which time slides were stained with DAPI and subjected to fluorescence microscopy.[51] Vector genome copy numbers were determined by qPCR using total

genomic DNA isolated from all of the tissues. The same tissue samples (20 mg each) were used for the isolation of total genomic DNA and RNA using the QIAmp DNA Mini Kit (catalog no. 51304) and RNeasy Plus Mini Kit (catalog no. 74134), respectively (Qiagen, Germantown, MD), followed by ProtoScript First Strand cDNA Synthesis Kit (New England Biolabs, Ipswich, MA) to generate cDNA from RNA extractions using 20 μg of total RNA. Delta-delta relative mRNA expression analysis was conducted using each sample's ΔCt = (hrGFP Ct – β-actin Ct). All of the organs were normalized individually, because RNA extraction efficiency can vary between cell types, to the respective average WT AAVrh74 ΔCt and reported as relative expression level, or $2^{-\Delta\Delta CT}$.

Statistical analyses

Results are presented as mean ± SEM. Differences between groups were identified using an unequal variance, 1-tailed distribution of the Student's t test. p values were considered significant under 0.05 and were represented as *$p < 0.05$ or **$p < 0.01$.

DATA AND CODE AVAILABILITY

All of the data will be made available upon reasonable request.

SUPPLEMENTAL INFORMATION

Supplemental information can be found online at https://doi.org/10.1016/j.omtm.2023.101147.

ACKNOWLEDGMENTS

This research was supported in part by Sarepta Therapeutics, National Institutes of Health grant nos. R01GM-119186 (to A.S.) and R21 AR-081018 (to A.S. and D.D.), the Children's Miracle Network, and the Kitzman Foundation (to A.S.).

AUTHOR CONTRIBUTIONS

J.S., K.Q., and G.D.K. designed and performed the experiments. J.S., K.Q., G.D.K., D.D., B.J.B., and A.S. analyzed the data. D.D., B.J.B., and A.S. conceived the idea. J.S. and A.S. wrote the manuscript, and all of the authors read and approved the final version.

DECLARATION OF INTERESTS

A.S. is a cofounder of, and has equity in, Lacerta Therapeutics. He also serves on the scientific advisory board of 4D Molecular Therapeutics. He is an inventor on several issued and filed patents on recombinant AAV vectors that have been or are being licensed to various AAV gene therapy companies. B.J.B. is an inventor of AAV-related patents that have been licensed to various AAV gene therapy companies. He is a co-founder and equity holder in Lacerta Therapeutics. D.D. is a member of the scientific advisory board for Solid Biosciences and equity holder in Solid Biosciences. He is also a member of the scientific advisory board of Sardocor Corporation. All of the other authors declare no competing interests.

REFERENCES

1. Wang, D., Tai, P.W.L., and Gao, G. (2019). Adeno-associated virus vector as a platform for gene therapy delivery. Nat. Rev. Drug Discov. *18*, 358–378.
2. Li, C., and Samulski, R.J. (2020). Engineering adeno-associated virus vectors for gene therapy. Nat. Rev. Genet. *21*, 255–272.
3. Mendell, J.R., Al-Zaidy, S.A., Rodino-Klapac, L.R., Goodspeed, K., Gray, S.J., Kay, C.N., Boye, S.L., Boye, S.E., George, L.A., Salabarria, S., et al. (2021). Current Clinical Applications of In Vivo Gene Therapy with AAVs. Mol. Ther. *29*, 464–488.
4. Keeler, A.M., and Flotte, T.R. (2019). Recombinant adeno-associated virus gene therapy in light of Luxturna (and Zolgensma and Glybera): Where are we, and how did we get here? (2019). Annu. Rev. Virol. *6*, 601–621.
5. Flotte, T.R., and Gao, G. (2020). Gene therapy enters its fourth decade. Hum. Gene Ther. *31*, 2–3.
6. Srivastava, A. (2016). Adeno-associated virus: The naturally occurring virus versus the recombinant vector. Hum. Gene Ther. *27*, 1–6.
7. Mingozzi, F., and High, K.A. (2011). High, K. Immune responses to AAV in clinical trials. (2011). Curr. Gene Ther. *11*, 321–330.
8. Verdera, H.C., Kuranda, K., and Mingozzi, F. (2020). AAV vector immunogenicity in humans: A long journey to successful gene transfer. Mol. Ther. *28*, 723–746.
9. Shieh, P.B., Bönnemann, C.G., Müller-Felber, W., Blaschek, A., Dowling, J.J., Kuntz, N.L., and Seferian, A.M. (2020). Letter to the Editor. Hum. Gene Ther. *31*, 787.
10. Duan, D. (2018). Micro-dystrophin gene therapy goes systemic in Duchenne muscular dystrophy patients. Hum. Gene Ther. *29*, 733–736.
11. Bowles, D.E., McPhee, S.W.J., Li, C., Gray, S.J., Samulski, J.J., Camp, A.S., Li, J., Wang, B., Monahan, P.E., Rabinowitz, J.E., et al. (2012). Phase 1 gene therapy for Duchenne muscular dystrophy using a translational optimized AAV vector. Mol. Ther. *20*, 443–455.
12. .https://www.solidbio.com/about/media/press-releases/solid-biosciences-reports-fourth-quarter-and-full-year-2021-financial-results-and-2-year-efficacy-and-safety-data-from-the-ongoing-phase-i-ii-ignite-dmd-clinical-trial-of-sgt-001.
13. Philippidis, A. (2022). After patient death, FDA places hold on Pfizer Duchenne muscular dystrophy gene therapy trial. Hum. Gene Ther. *33*, 111–115.
14. Lek, A., Wong, B., Keeler, A., Blackwood, M., Ma, K., Huang, S., Sylvia, K., Batista, A.R., Artinian, R., Kokoski, D., et al. (2023). Death after high-dose rAAV9 gene therapy in a patient with Duchenne muscular dystrophy. N. Engl. J. Med. *389*, 1203–1210.
15. Mullard, A. (2021). Sarepta's DMD gene therapy falls flat. Nat. Rev. Drug Discov. *20*, 91.
16. .https://www.fda.gov/vaccines-blood-biologics/tissue-tissue-products/elevidys.
17. Zhong, L., Li, B., Mah, C.S., Govindasamy, L., Agbandje-McKenna, M., Cooper, M., Herzog, R.W., Zolotukhin, I., Warrington, K.H., Jr., Weigel-Van Aken, K.A., et al. (2008). Next generation of adeno-associated virus 2 vectors: point mutations in tyrosines lead to high-efficiency transduction at lower doses. (2008). Proc. Natl. Acad. Sci. USA *105*, 7827–7832.
18. Markusic, D.M., Herzog, R.W., Aslanidi, G.V., Hoffman, B.E., Li, B., Li, M., Jayandharan, G.R., Ling, C., Zolotukhin, I., Ma, W., et al. (2010). High-efficiency transduction and correction of murine hemophilia B using AAV2 vectors devoid of multiple surface-exposed tyrosines. Mol. Ther. *18*, 2048–2056.
19. Martino, A.T., Basner-Tschakarjan, E., Markusic, D.M., Finn, J.D., Hinderer, C., Zhou, S., Ostrov, D.A., Srivastava, A., Ertl, H.C.J., Terhorst, C., et al. (2013). Engineered AAV vector minimizes in vivo targeting of transduced hepatocytes by capsid-specific $CD8^+$ T cells. Blood *121*, 2224–2233.
20. Ling, C., Wang, Y., Lu, Y., Wang, L., Jayandharan, G.R., Aslanidi, G.V., Li, B., Cheng, B., Ma, W., Lentz, T., et al. (2015). Enhanced transgene expression from recombinant single-stranded D-sequence-substituted adeno-associated virus vectors in human cell lines in vitro and in murine hepatocytes in vivo. J. Virol. *89*, 952–961.
21. Ling, C., Li, B., Ma, W., and Srivastava, A. (2016). Development of optimized AAV serotype vectors for high-efficiency transduction at further reduced doses. Hum. Gene Ther. Methods *27*, 143–149.
22. Aslanidi, G.V., Rivers, A.E., Ortiz, L., Song, L., Ling, C., Govindasamy, L., Van Vliet, K., Tan, M., Agbandje-McKenna, M., and Srivastava, A. (2013). Optimization of the capsid of recombinant adeno-associated virus 2 (AAV2) vectors: The final threshold? PLoS One *8*, e59142.
23. Potter, R.A., Griffin, D.A., Heller, K.N., Peterson, E.L., Clark, E.K., Mendell, J.R., and Rodino-Klapac, L.R. (2021). Dose-escalation study of systemically delivered

rAAVrh74.MHCK7.micro-dystrophin in the mdx mouse model of Duchenne muscular dystrophy. Hum. Gene Ther. *32*, 375–389.

24. Zhong, L., Li, B., Jayandharan, G., Mah, C.S., Govindasamy, L., Agbandje-McKenna, M., Herzog, R.W., Weigel-Van Aken, K.A., Hobbs, J.A., Zolotukhin, S., et al. (2008). Tyrosine-phosphorylation of AAV2 vectors and its consequences on viral intracellular trafficking and transgene expression. Virology *381*, 194–202.
25. Ling, C., Li, J., Zhang, D., Aslanidi, G., Ling, C., and Srivastava, A. (2016). The role of glucocorticoid receptor signaling in adeno-associated virus 2 infection. Mol. Ther. *24*, S6.
26. Mah, C., Qing, K., Khuntirat, B., Ponnazhagan, S., Wang, X.-S., Kube, D.M., Yoder, M.C., and Srivastava, A. (1998). Adeno-associated virus type 2-mediated gene transfer: role of epidermal growth factor receptor protein tyrosine kinase in transgene expression. J. Virol. *72*, 9835–9843.
27. Srivastava, A. (2020). AAV Vectors: Are they safe? Hum. Gene Ther. *31*, 697–699.
28. Sender, R., Fuchs, S., and Milo, R. (2016). Revised estimates for the number of human and bacteria cells in the body. PLoS Biol. *14*, e1002533.
29. Mendell, J.R., Sahenk, Z., Lehman, K., Nease, C., Lowes, L.P., Miller, N.F., Iammarino, M.A., Alfano, L.N., Nicholl, A., Al-Zaidy, S., et al. (2020). Assessment of Systemic delivery of rAAVrh74.MHCK7.micro-dystrophin in children with Duchenne muscular dystrophy: A nonrandomized controlled trial. JAMA Neurol. *77*, 1122–1131.
30. Broomfield, J., Hill, M., Guglieri, M., Crowther, M., and Abrams, K. (2021). Life expectancy in Duchenne muscular dystrophy: Reproduced individual patient data meta-analysis. Neurol. *97*, e2304–e2314.
31. Duan, D., Goemans, N., Takeda, S., Mercuri, E., and Aartsma-Rus, A. (2021). Duchenne muscular dystrophy (2021). Nat. Rev. Dis. Prim. *7*, 13.
32. Weinmann, J., Weis, S., Sippel, J., Tulalamba, W., Remes, A., El Andari, J., Herrmann, A.K., Pham, Q.H., Borowski, C., Hille, S., et al. (2020). Identification of a myotropic AAV by massively parallel in vivo evaluation of barcoded capsid variants. Nat. Commun. *11*, 5432.
33. El Andari, J., Renaud-Gabardos, E., Tulalamba, W., Weinmann, J., Mangin, L., Pham, Q.H., Hille, S., Bennett, A., Attebi, E., Bourges, E., et al. (2022). Semirational bioengineering of AAV vectors with increased potency and specificity for systemic gene therapy of muscle disorders. Sci. Adv. *8*, eabn4704.
34. Tabebordbar, M., Lagerborg, K.A., Stanton, A., King, E.M., Ye, S., Tellez, L., Krunnfusz, A., Tavakoli, S., Widrick, J.J., Messemer, K.A., et al. (2021). Directed evolution of a family of AAV capsid variants enabling potent muscle-directed gene delivery across species. Cell *184*, 4919–4938.e22.
35. Manno, C.S., Pierce, G.F., Arruda, V.R., Glader, B., Ragni, M., Rasko, J.J., Ozelo, M.C., Hoots, K., Blatt, P., Konkle, B., et al. (2006). Successful transduction of liver in hemophilia by AAV-Factor IX and limitations imposed by the host immune response. Nat. Med. *12*, 342–347.
36. Nathwani, A.C., Tuddenham, E.G.D., Rangarajan, S., Rosales, C., McIntosh, J., Linch, D.C., Chowdary, P., Riddell, A., Pie, A.J., Harrington, C., et al. (2011). Adenovirus-associated virus vector-mediated gene transfer in hemophilia B. (2011). N. Engl. J. Med. *365*, 2357–2365.
37. Nathwani, A.C., Reiss, U.M., Tuddenham, E.G.D., Rosales, C., Chowdary, P., McIntosh, J., Della Peruta, M., Lheriteau, E., Patel, N., Raj, D., et al. (2014). Long-term safety and efficacy of factor IX gene therapy in hemophilia B. (2014). N. Engl. J. Med. *371*, 1994–2004.
38. Konkle, B.A., Walsh, C.E., Escobar, M.A., Josephson, N.C., Young, G., von Drygalski, A., McPhee, S.W.J., Samulski, R.J., Bilic, I., de la Rosa, M., et al. (2021). BAX 335 hemophilia B gene therapy clinical trial results: potential impact of CpG sequences on gene expression. Blood *137*, 763–774.
39. https://investors.adverum.com/news/news-details/2021/Adverum-Provides-Update-on-ADVM-022-and-the-INFINITY-Trial-in-Patients-with-Diabetic-Macular-Edema/default.aspx.
40. https://4dmt.gcs-web.com/news-releases/news-release-details/4d-molecular-therapeutics-reports-interim-results-4d-310-phase.
41. https://sparktx.com/press_releases/spark-therapeutics-updated-spk-8011-data-from-phase-1-2-study-shows-multi-year-durable-factor-viii-fviii-expression-that-significantly-reduced-bleeding-in-hemophilia-a-patients/.
42. https://www.fiercebiotech.com/biotech/fda-puts-logicbio-genome-editing-therapy-trial-hold-after-second-infant-suffers-adverse.
43. Srivastava, A. (2023). Rationale and strategies for the development of safe and effective optimized AAV vectors for human gene therapy. Mol. Ther. Nucleic Acids *32*, 949–959.
44. Wang, W., and Malcolm, B.A. (1999). Two-stage PCR protocol allowing introduction of multiple mutations, deletions and insertions using QuikChange Site-Directed Mutagenesis. Biotechniques *26*, 680–682.
45. Kube, D.M., and Srivastava, A. (1997). Quantitative DNA slot blot analysis: inhibition of DNA binding to membranes by magnesium ions. Nucleic Acids Res. *25*, 3375–3376.
46. Wang, Y., Ling, C., Song, L., Wang, L., Aslanidi, G.V., Tan, M., Ling, C., and Srivastava, A. (2012). Limitations of encapsidation of recombinant self-complementary adeno-associated viral genomes in different serotype capsids and their quantitation. Hum. Gene Ther. Methods *23*, 225–233.
47. Rambhai, H.K., Ashby, F.J., 3rd, Qing, K., and Srivastava, A. (2020). Role of essential metal ions in AAV vector-mediated transduction (2020). Mol. Ther. Meth. Clin. Dev. *18*, 159–166.
48. Yang, H., Qing, K., Keeler, G.D., Yin, L., Mietzsch, M., Ling, C., Hoffman, B.E., Agbandje-McKenna, M., Tan, M., Wang, W., and Srivastava, A. (2020). Enhanced transduction of human hematopoietic stem cells by AAV6 vectors: Implications in gene therapy and genome editing. Mol. Ther. Nucleic Acids *20*, 451–458.
49. Zhong, L., Qing, K., Si, Y., Chen, L., Tan, M., and Srivastava, A. (2004). Heat-shock treatment-mediated increase in transduction by recombinant adeno-associated virus 2 vectors is independent of the cellular heat-shock protein 90. J. Biol. Chem. *279*, 12714–12723.
50. Zhong, L., Zhao, W., Wu, J., Li, B., Zolotukhin, S., Govindasamy, L., Agbandje-McKenna, M., and Srivastava, A. (2007). A dual role of EGFR protein tyrosine kinase signaling in ubiquitination of AAV2 capsids and viral second-strand DNA synthesis. Mol. Ther. *15*, 1323–1330.
51. Shoti, J., Qing, K., and Srivastava, A. (2022). Development of an AAV DNA-based synthetic vector for the potential gene therapy of hemophilia in children. Front. Microbiol. *13*, 1033615.